Mössbauer spectroscopic study of heat-treated and control-cooled Fe_3Al alloys

D. BANDYOPADHYAY*, S. SUWAS**, R. M. SINGRU*, S. BHARGAVA**
** Department of Physics, and ** Department of Materials and Metallurgical Engineering, Indian Institute of Technology, Kanpur - 208 016 India*

The Fe–Al system forms a model object of transition metal-sp element system. Fe–Al alloys containing 21–31 at % Al are known to exhibit several attractive physical properties which render them candidate materials for structural and magnetic applications. These magnetic and physical properties can be varied by altering the composition and the processing routes. Keeping this in mind, Mössbauer spectra of five Fe–24 at % Al and Fe–25 at % Al alloy samples processed via different routes have been studied. The analysis of the Mössbauer parameters, distribution of hyperfine magnetic fields, P(H) and H-values were used to identify various Fe-atom configurations (nearest neighbour or next nearest neighbour) associated with the phases formed by different processing routes. The results obtained from the present study indicate that the average hyperfine field $\langle H \rangle$ depends on the average rate of cooling followed during the precipitation of these phases.

1. Introduction

Fe–Al alloys containing 22–31 at % Al are known to exhibit several attractive properties which render them potential materials for structural and magnetic applications. These alloys possess a high strength, low density and extremely good corrosion and oxidation resistance which make them suitable materials for structural applications [1]. Regarding their magnetic properties, their high magnetic permeability and large magnetostriction qualify these alloys as important materials useful for technological applications [2]. Further it is observed that a series of Fe–Al alloys that possess different soft magnetic and physical properties can be obtained by varying the composition and the process of heat treatment [2].

For example the Fe–22 at % Al alloy has a high magnetic permeability induction, the Fe–25 at % Al alloy has a large magnetostriction whilst the Fe–28 at % Al alloy possess a high magnetic permeability. These three alloys have emerged as important materials that find use in a wide range of engineering applications [2]. Although the Al-concentration in these three alloys does not differ much, the processing routes by which they are heat-treated and cooled for practical use differ significantly. The variations in the magnetic properties of these Fe–Al alloys are thought to arise from the different atomic configurations in their crystal structure [3]. It has been recognized that ^{57}Fe Mössbauer spectroscopy offers a sensitive microscopic point-probe to identify the nature of the ^{57}Fe-atom configurations responsible for different hyperfine fields, H, observed in iron-based alloys [4–11]. Other possible techniques available for the study of atomic configurations are transmission electron microscopy (TEM) and X-ray diffraction (XRD). The former technique, TEM, provides only a localized probe while the latter technique (XRD) suffers from drawbacks that limit its application to the present problem. These drawbacks arise because superlattice reflections are very weak in intensity and the changes in the lattice parameters for fundamental reflections introduce complications into the data analysis. Again the sensitivity of each technique to bulk effects is different. Considering all these aspects, Mössbauer spectroscopy is the best and most sensitive technique to identify different phases (arising out of different atomic configurations) and to estimate their volume fractions. Although the Fe–Al system has been extensively studied using ^{57}Fe Mössbauer spectroscopy, most of the investigations have been carried out in order to examine the effect of either the composition or the heat treatment temperature of the sample [4–11]. Few studies have attempted to measure the Mössbauer spectra at room temperature keeping the composition fixed but using different processing routes (i.e. heat-treatments and cooling modes) for the samples.

The Fe–Al system is characterized by a wide range of α-Fe solid solution upto 22 at % Al at room temperature. On increasing the Al content further a number of intermetallic phases: Fe_3Al, FeAl, $FeAl_2$, Fe_2Al_5 and $FeAl_3(Fe_4Al_{13})$ are exhibited. The magnetic moment of the Fe atoms is almost the same as in α-Fe [12]. The Mössbauer spectra observed for these alloys closely resemble that of α-Fe with some minor differences [4]. The alloys containing more than $\sim$32 at % Al form the ordered B2 or CsCl structure and are nonmagnetic. Their structure consists of two

0022–2461

interpenetrating simple cubic lattices, one of pure Fe and the other of pure Al. On the other hand the structure of the alloys having ~18–32 at % Al is complicated and cannot be described in a straightforward manner. Mössbauer spectra for this series of alloys show a complex nature which appears to strongly depend on the history and heat-treatment of the samples. Analysing these spectra into constituent subspectra and identifying them has been a challenging problem in Mössbauer spectroscopy [13]. Keeping these aspects in mind, in the present investigation, the effect of the quenching or cooling process (involved during the sample preparation) on the hyperfine magnetic field H present in various phases due to Fe sites having different Fe atom configurations have been studied using ^{57}Fe Mössbauer spectroscopy. The phases were produced either through equilibrium slow cooling or by rapid quenching involving a schedule described in the next section. The composition of the alloys was chosen with the aim of bringing the cooling path through the triangular region of the phase diagram (Fig. 1). By varying the temperatures, these alloys pass through regions of different phase fields (Fig. 1), that by following proper heat treatment and cooling mode, the volume fraction of different phases can be suppressed, retained or allowed to grow.

2. Experimental procedure

The Fe–Al alloys were prepared from high purity Fe and Al metals having 99.99% purity by consumable electrode arc melting in a water-cooled copper crucible. The ingots were homogenized at 1000 °C for 168 h in order to remove any compositional inhomogeneity. The homogeneity was checked by characterizing the homogenized alloys using an electron probe analyser (Table 1). Small pieces of the homogenized ingots were cut and encapsulated in quartz capsules in a high vacuum (1.333×10^{-4} Pa). These capsules were then heat treated in a vertical tube furnace by following the processing schedule shown in Table II. The samples for Mössbauer spectroscopy were prepared from powdered (particle size less than 53 μm) samples of these five alloys (designated as FA1–FA5, see Table II) and they were used to record transmission Mössbauer spectra at room temperature (23 °C). The spectra were obtained using Mössbauer spectrometer coupled to a multichannel analyser and operated in a constant acceleration mode. A ^{57}Co source embedded in a rhodium matrix (Amersham International Ltd., Amersham, UK) was used and the spectrometer was calibrated using a standard α-Fe foil.

TABLE I Chemical compositions of the two Fe–Al alloys studied measured using the electron probe microanalyser

Alloy	Average composition (at %)	
	Fe	Al
1	76.1	23.9
2	74.7	25.3

The analysis of the Mössbauer spectra was carried out with computer programs using two methods. In the first method a least-squares-fitting computer program employing Lorentzian shapes for the peaks and an iterative procedure was used. It was assumed that the total Mössbauer spectrum was a superposition of a number of contributing subspectra each having different Mössbauer parameters (i.e., hyperfine field H, isomer shift IS, relative intensity etc).

In the second method we followed the procedure of Window [14] to obtain the hyperfine field distributions, $P(H)$, and the average hyperfine field, $\langle H \rangle = \int HP(H)\,dH / \int P(H)\,dH$.

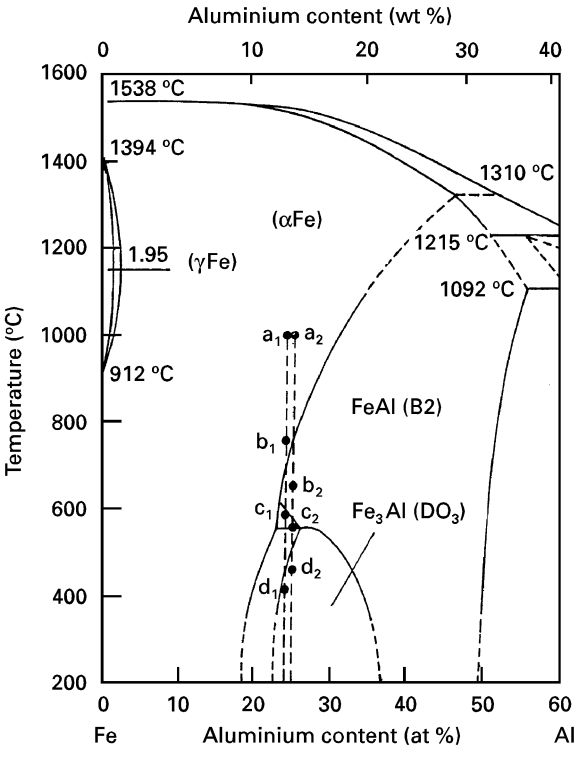

Figure 1 Iron rich portion of the Fe–Al phase diagram [12].

3. Results and discussion

3.1. Analysis using least-squares-fitting to the Mössbauer spectra

Mössbauer spectra observed for the five different samples FA1–FA5 (Table II) at room temperature are shown in Fig. 2(a–e) respectively and they appear to be similar. Each of these spectra was found to be complex and could be decomposed into five sextets (subspectra) without any trace of a paramagnetic component.

The hyperfine magnetic fields, H, obtained for each of these subspectra are listed in Table III. The width of the lines in each of these subspectra appeared broader, showing full width at half maximum (FWHM) values in the range of 0.35–0.40 mm s^{-1} as compared to the value of 0.25 mm s^{-1} observed for pure α-Fe. It is interesting to note that for the Fe–5.1 at % Al alloy Stearns [4] has also observed five values of the hyperfine field H. To facilitate a comparison of the five

TABLE II Routes and heat-treatment schedules and processing of the Fe–Al alloys. See Fig. 1 for an explanation of the symbols a_1, b_1, etc. used to describe the synthesis route

Sample	Composition	Route used for heat treatment and processing
FA1	Fe–24 at % Al	*Route* 1: $a_1 \rightarrow$ ice quenching As-cast alloy was heated at 1000 °C for 168 h. It was then ice quenched from the disordered α-phase field
FA2	Fe–24 at % Al	*Route* 2: $a_1 \rightarrow b_1 \rightarrow$ ice quenching As-cast alloy was heated at 1000 °C for 168 h. It was then cooled from 1000 to 750 °C at a rate of 2 °C min^{-1}. After keeping it at 750 °C for 48 h, it was ice quenched.
FA3	Fe–24 at % Al	*Route* 3: $a_1 \rightarrow b_1 \rightarrow c_1 \rightarrow$ ice quenching As-cast alloy was heated at 1000 °C for 168 h. It was then cooled from 1000 to 750 °C at a rate of 2 °C min^{-1}. Then it was cooled from 750 to 575 °C at a rate of 2 °C min^{-1}. After keeping it at 575 °C for 48 h, it was ice-quenched from the triple phase field α, B2 and DO_3.
FA4	Fe–24 at % Al	*Route* 4: $a_1 \rightarrow b_1 \rightarrow c_1 \rightarrow d_1 \rightarrow$ cooled to RT As-cast alloy was heated at 1000 °C for 168 h. It was then cooled from 1000 to 750 °C at a rate of 2 °C min^{-1}. Then it was cooled from 750 to 575 °C at a rate of 2 °C min^{-1}. It was kept at 575 °C for 48 h and was then cooled to 400 °C at 2 °C min^{-1}. It was then furnace cooled to room temperature from the DO_3 phase field.
FA5	Fe–25 at % Al	*Route* 5: $a_2 \rightarrow b_2 \rightarrow c_2 \rightarrow d_2 \rightarrow$ cooled to RT As-cast alloy was heated at 1000 °C for 168 h. It was then cooled at a rate of 1 °C min to 650 °C to the imperfectly ordered B2 phase. Then it was cooled to 550 °C and held for 6 h to ensure the transformation from the B2 $\rightarrow$ DO_3 phase. It was then cooled to 450 °C at a rate of 1 °C min^{-1} and held at 450 °C for 48 h in order to stabilize the DO_3 phase. Then it was slowly cooled to RT.

H-values observed in the present investigation for each of the different samples, they have been plotted in Fig. 3 in such a manner that each vertical column shows the *H*-values obtained for a particular sample. It is observed that the set of *H*-values observed for the first four samples FA1, FA2, FA3 and FA4 (all containing 24 at % Al) agree among each other within the experimental error. The *H*-values for the Fe–25 at % Al alloy (sample FA5), however, shows a different set. This aspect will be discussed later.

It is observed from Table III that the subspectra yield *H*-values lying in the range $H = 318$–197 kOe (where 1oe = 79.58 Am^{-1}). Using Mössbauer spectroscopy, Stearns [4] has shown how the hyperfine magnetic field *H* at the Fe nuclei in Fe–Al alloys depends upon the number of Al atoms in the surrounding co-ordination spheres. A similar approach has been used by other workers [5–11] to explain their hyperfine magnetic fields observed by Mössbauer spectroscopy in the Fe–Al system. Stearns [4] interpreted his data in terms of the effect of solute atoms in the first five neighbour shells whilst Perez Alcazar and Galvao da Silva [10] considered the effect of only the first (nearest neighbour nn) and second (next nearest neighbour nnn) neighbouring shells. These workers assumed that the 8Fe nn + 6Fe nnn configuration gives a H_0 value of 330 kOe however this field is reduced to $H = H_o - n_1\Delta H_1 - n_2\Delta H_2$ where n_1 and n_2 are the number of Al atoms in the 8 nearest (nn) and the 6 next nearest (nnn) neighbouring sites to Fe. Following Stearns [4] they initially used a ΔH_1 value of 24 kOe (which is the reduction in *H* for each Fe atom substituted by an Al in the nn site) and a ΔH_2 value of 11 kOe (which is the reduction in *H* for each Fe atom substituted by an Al in the nnn site). The probability of finding n_1 Al atoms in the first Fe shell and n_2 in the second Fe shell is given by the binomial distribution [10]:

$$P(n_1, n_2) = C_8^{n_1} C_6^{n_2} q^{n_1+n_2}(1-q)^{14-n_1-n_2} \qquad (1)$$

where q is the Al concentration and C_i^j are the binomial coefficients.

In order to interpret their experimental data, Perez Alcazar and Galvao da Silva [10] applied another empirical relation:

$$H = H_0(1 - \alpha n_1 - \beta n_2) \qquad (2)$$

where H_o has a value of 330 kOe, α is the value corresponding to an ΔH_1 value of 24 kOe (in agreement with Stearns [4]) and $\beta = 1.5\%$ (which gave a ΔH_2 value of 5 kOe). Yeluskov *et al.* [11] only considered the effects of nn atoms and found that the local hyperfine field *H* depended nonlinearly on the number of nn Al atoms, the fourth and next (upto eight) nn atoms caused *H* to change by a greater extent than the first three atoms.

In order to facilitate the interpretation of the present results (Table III) we have collated the values of *H* predicted by the above three different models in Table IV. Additional experimental results are also included in Table IV for the sake of completeness.

The data presented in Table IV have been used to propose assignments for the Fe-atom configurations responsible for producing each of the five subspectra observed in the present work. In making these assignments the following factors were considered: (i) the models used in the present investigation in the preparation of Table IV are empirical in nature and thus the values of the parameters ΔH_1, ΔH_2, α and β are only approximate in nature. (ii) The values stated for various parameters in the literature [4–11] are by no

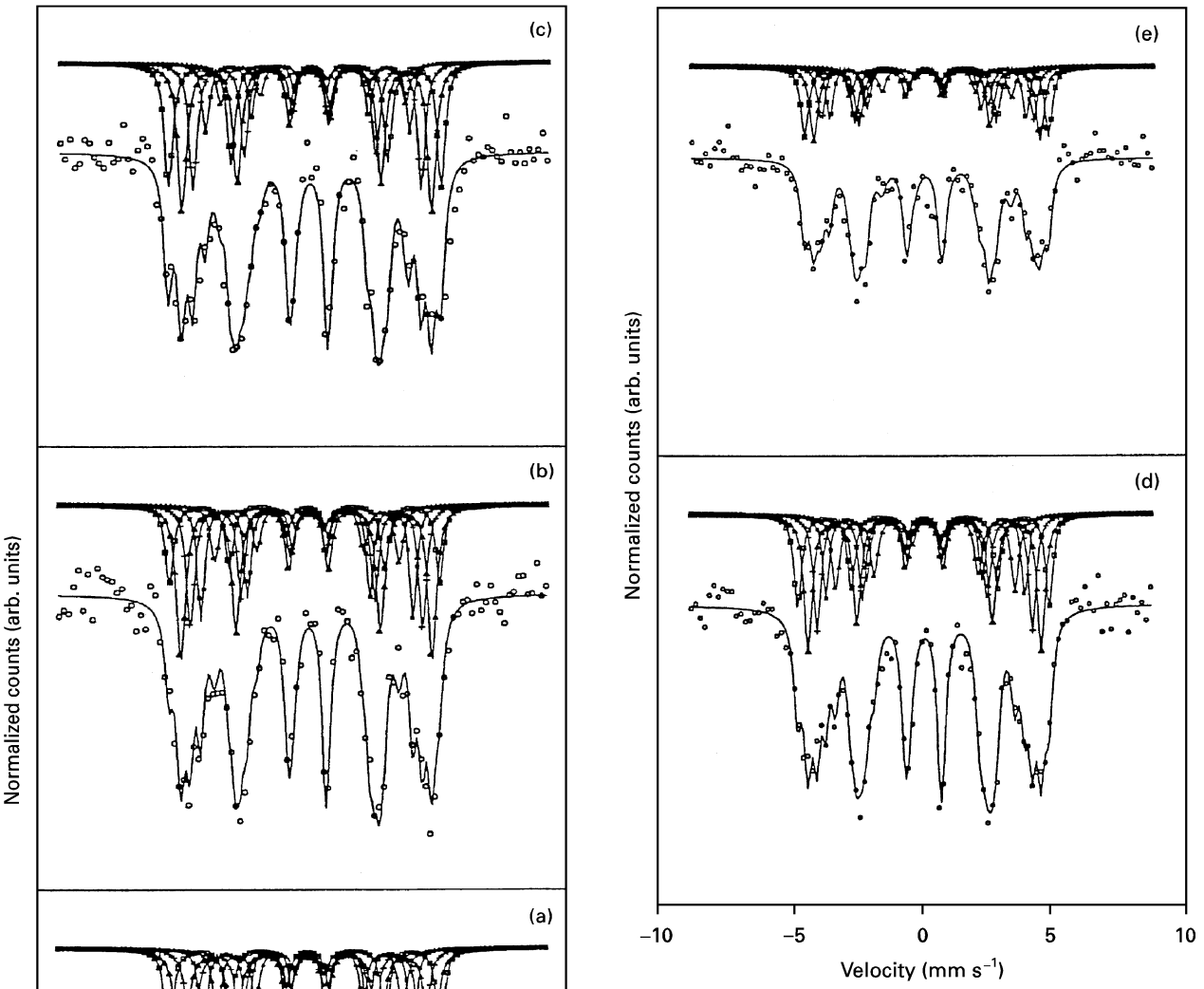

Figure 2 Mössbauer spectra of Fe–Al samples, (a) FA1, (b) FA2, (c) FA3, (d) FA4 and (e) FA5. Open circles (lower spectrum) represent the experimental data points. The upper plot shows the five subspectra providing the best fit with (□), (△), (+), (■) and (▲) representing sites I, II, III, IV and V (see Table III) respectively.

means unique and the situation in this regard is not completely clear yet. Nevertheless these models provide an existing basis for identifying the configurations responsible for each H-value.

The results obtained for each sample are discussed separately in the following subsections.

3.1.1. Sample FA1; Fe–24 at % Al

The highest value for the hyperfine magnetic field, H, observed for the FA1 sample is 310 ± 4 kOe and this has been assigned to a configuration around the Fe atom of (7Fe + 1Al) nn + 6Fe nnn (i.e., one in which one nn Fe atom is replaced by one Al atom). It can be seen from Table IV that a 8 Fe nn + (4Fe + 2Al) nnn configuration could also possibly exist, however, with a lower probability. The second H value, 286 ± 4 kOe is attributed to a configuration of (6Fe + 2Al) nn + 6 Fe nnn along with a possible 8Fe nn + (2Fe + 4Al) nnn configuration which again exists with a lower probability. The assignments for the other 3 values, 269 ± 4, 240 ± 4 and 214 ± 4 kOe are as listed in Table III. It should be noted that if the possibility of Al atoms occupying the nnn sites is excluded, the assignments for the five H-values for FA1 fall in the pattern $(8 - n_1)$ Fenn + n_1Al nn + 6Fe nnn, with $n_1 = 1$, 2, 3, 4 and 5 respectively. Considering the straightforward nature of route 1 in which the sample was ice-quenched from the disordered α-phase at 1000 °C, and in which the retention of the α-phase is expected to occur, the above pattern might be possible.

TABLE III Mössbauer parameters (H, Γ, intensity) of the FA1–FA5 samples measured at room temperature along with the proposed assignment of configurations that produce the hyperfine magnetic fields

Sample	Site	H[(a)] $\times 79.58 \times 10^3$ (Am^{-1})	Γ[(b)]	Intensity[(c)] (%)	Assignment[(d)]
FA1	I	310	0.37	17	(7Fe + 1Al) nn + 6Fe nnn and 8Fe nn + (4Fe + 2Al) nnn
	II	286	0.38	31	(6Fe + 2Al) nn + 6Fe nnn and 8Fe nn + (2Fe + 4Al) nnn
	III	264	0.37	24	(5Fe + 3Al) nn + 6Fe nnn and 8Fe nn + 6Al nnn
	IV	240	0.30	15	(4Fe + 4Al) nn + 6Fe nnn
	V	214	0.38	13	(3Fe + 5Al) nn + 6Fe nnn
FA2	I	309	0.36	15	(7Fe + 1Al) nn + 6Fe nnn and 8Fe nn + (4Fe + 2Al) nnn
	II	288	0.38	32	(6Fe + 2Al) nn + 6Fe nnn and 8Fe nn + (2Fe + 4Al) nnn
	III	266	0.34	22	(5Fe + 3Al) nn + 6Fe nnn and 8Fe nn + 6Al nnn
	IV	243	0.31	19	(4Fe + 4Al) nn + 6Fe nnn
	V	212	0.38	12	(3Fe + 5Al) nn + 6Fe nnn
FA3	I	311	0.36	25	(7Fe + 1Al) nn + 6Fe nnn and 8Fe nn + (4Fe + 2Al) nnn
	II	286	0.38	31	(6Fe + 2Al) nn + 6Fe nnn and 8Fe nn + (2Fe + 4Al) nnn
	III	261	0.34	23	(5Fe + 3Al) nn + 6Fe nnn and 8Fe nn + 6Al nnn
	IV	234	0.31	12	(4Fe + 4Al) nn + 6Fe nnn
	V	213	0.38	9	(3Fe + 5Al) nn + 6Fe nnn
FA4	I	304	0.36	19	(7Fe + 1Al) nn + 6Fe nnn and 8Fe nn + (4Fe + 2Al) nnn
	II	282	0.38	29	(6Fe + 2Al) nn + 6Fe nnn and 8Fe nn + (2Fe + 4Al) nnn
	III	260	0.34	22	(5Fe + 3Al) nn + 6Fe nnn and 8Fe nn + 6Al nnn
	IV	241	0.31	14	(4Fe + 4Al) nn + 6Fe nnn
	V	217	0.38	16	(3Fe + 5Al) nn + 6Fe nnn
FA5	I	295	0.36	25	8Fe nn + (3Fe + 3Al) nnn
	II	273	0.38	28	8Fe nn + (1Fe + 5Al) nnn
	III	257	0.34	18	(5Fe + 3Al) nn + 6Fe nnn and 8Fe nn + 6Al nnn
	IV	237	0.31	17	(4Fe + 4Al) nn + 6Fe nnn
	V	194	0.38	12	(2Fe + 6Al) nn + 6Fe nnn

(a) H = Hyperfine magnetic field at the ^{57}Fe nucleus. Typical error is $\pm 4 \times 79.58 \times 10^3$ Am^{-1}.
(b) Γ (FWHM) is the full width at half maximum of the spectral line values in $mm\,s^{-1}$. Typical error is ± 0.01 $mm\,s^{-1}$
(c) The area values are given as percentages. Typical error is ± 1 (%)
(d) Proposed Fe atom configuration: nn = nearest neighbour, nnn = next nearest neighbour

3.1.2. FA2 to FA4 samples: Fe–24 at % Al

The H-values determined for these three samples agree, within experimental error, with those obtained for the FA1 sample although the relative intensities are different. This indicates that going down the vertical line in the phase diagram shown in Fig. 1 from a_1 to b_1, the same configurations are formed although their relative population is determined by the intermediate heat treatments and cooling rate and other details of the processing route.

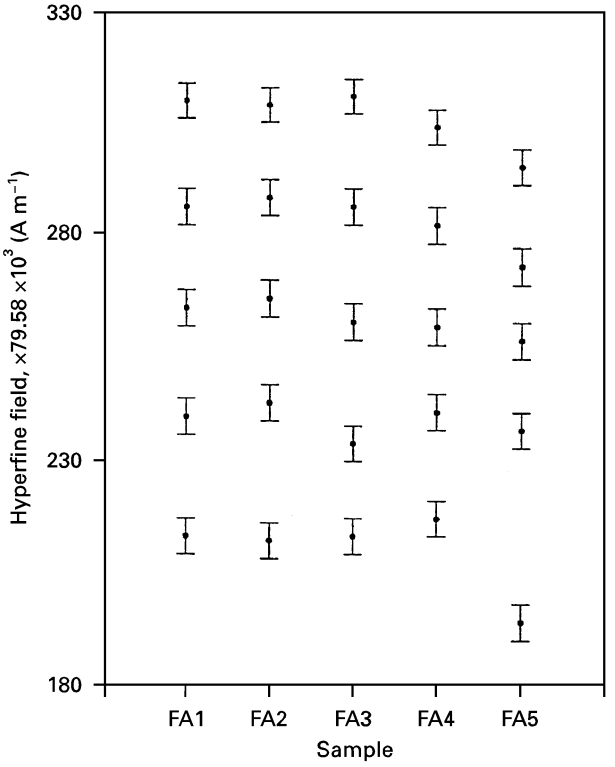

Figure 3 Variation of the hyperfine field for different sites in samples FA1–FA5.

3.1.3. FA5 sample; Fe–25 at % Al

The H-values obtained for this sample are 295 ± 4, 273 ± 4, 257 ± 4, 237 ± 4 and 194 ± 4 kOe. While the two values, namely 257 ± 4 and 237 ± 4 kOe, agree with those obtained for samples FA1–FA4 within experimental error, the other three H-values are different. This suggests that sample FA5 that has a different (25 at % Al compared to 24 at % Al of samples FA1–FA4) composition and was processed via a more elaborate processing route has different configurations, as shown in Table III. The ratio of the intensities for the configurations giving rise to the H values 257 ± 4 and 237 ± 4 kOe is ~ 1 for the FA5 sample while it is in the range ~ 1.2–1.5 for samples FA1–FA4 respectively. The linewidths for the 5 subspectra of each sample follows a similar pattern, with the (4Fe + 4Al) nn + 6Fe nnn showing an approximately 20% smaller value compared to other configurations.

3.2. Analysis using the method of Window [14]

Previous studies [10, 11] of the hyperfine fields in Fe–Al alloys have shown that the behaviour of the average hyperfine field, $\langle H \rangle$, provides useful information. While the individual H-values (the five values determined in Table III) are seen at a microscopic scale through the Mössbauer effect, in other phenomena the average field $\langle H \rangle$, seen on a macroscopic scale, could become more important. One method of

TABLE IV Magnetic hyperfine field values for different Fe atom configurations in the Fe–Al alloys reported in the literature

Label	Configuration	Magnetic hyperfine field $\times 79.58 \times 10^3$ (Am^{-1})			
		[4][a]	[10][b]	[11][c]	Others
1.	8Fe nn + 6Fe nnn	330	330	330	
2.	(7Fe + 1Al) nn + 6Fe nnn	306	306	312	
3.	(6Fe + 2Al) nn + 6Fe nnn	282	282	288	
4.	(5Fe + 3Al) nn + 6Fe nnn	258	258	264	261[d]
5.	(4Fe + 4Al) nn + 6Fe nnn	234	234	229	230[e]
6.	(3Fe + 5Al) nn + 6Fe nnn	210	210	167	
7.	(2Fe + 6Al) nn + 6Fe nnn	186	186	122	
8.	(1Fe + 7Al) nn + 6Fe nnn	162	162	65	
9.	8Fe nn + (5Fe + 1Al) nnn	319	325		
10.	8Fe nn + (4Fe + 2Al) nnn	308	320		
11.	8Fe nn + (3Fe + 3Al) nnn	297	315		
12.	8Fe nn + (2Fe + 4Al) nnn	286	310		
13.	8Fe nn + (1Fe + 5Al) nnn	275	305		
14.	8Fe nn + 6Al nnn (DO3)	264	300		300[e]

(a) Calculated with $\Delta H_1 = 24$ kOe, $\Delta H_2 = 11$ kOe (1Oe = 79.58 Am^{-1})
(b) Calculated with $\Delta H_1 = 24$ kOe, $\Delta H_2 = 5$ kOe (1Oe = 79.58 Am^{-1})
(c) Reference [11]
(d) Reference [8]
(e) Reference [3]

determining $\langle H \rangle$ is to use the relation:

$$\langle H \rangle = \int HP(H)\,dH \Big/ \int P(H)\,dH \qquad (3)$$

where $P(H)$ is the function describing the hyperfine field distribution. For this the Mössbauer spectra of the FA1–FA5 samples have been analysed using the previously discussed method of Window [14]. The calculated $P(H)$ distributions are presented in Fig. 4 while the values of $\langle H \rangle$ calculated with Equation 3 are listed in Table V. Also listed in Table V are the values of the single average isomer shift (or $\langle$IS$\rangle$) relative to α-Fe obtained for the five samples.

The $P(H)$ distributions, Fig. 4, do not exhibit any sharp profiles but they do however, all show a broad inverted bell-type shape. The broad and asymmetric nature of these distributions suggest their composite nature of being built from the distributions contributed by each of the five H-values (Table III). It is interesting to point out that the hyperfine field distributions obtained by Perez Alcazar and Galvao de Silva [10] for $Fe_{1-q}Al_q$ (q = 0.15, 0.2 and 0.225) and by Yeluskov et al. [11] for Fe–23.5 at % Al showed similar shapes. Furthermore the value of $\langle H \rangle$ obtained [10] for $Fe_{1-q}Al_q$ decreased from an $\langle H \rangle$ value of 323.95 kOe for q = 0.025 to 272.10 kOe for q = 0.225. In the present case the $P(H)$ distributions for the FA1, FA2, FA3 and FA4 samples were asymmetrical with the ratio of the halfwidths at half maximum, ΔH_1 (on the left side): ΔH_2 (on the right side) being about 1.35. On the other hand the dominant peak in the $P(H)$ for the FA5 sample is fairly symmetrical although it shows a broad bulge in the lower (H = 145–190 kOe) field region. It may be pointed out that the least-squares-fitting analysis (Table III) did not yield any H-value lower than 194 kOe. The values of H_{peak} (the most probable value of H) as well as those of $\langle H \rangle$ appear to decrease in the sequence FA1 to FA5 although the average values of the isomer shift $\langle IS \rangle$ remain constant. Although the variations of the cooling rates involved in the process routes 1 to 5 (Table II) cannot be described by a single parameter, an examination of Table II indicates that the average rate of cooling is different for the five samples and that it decreases in the sequence FA1, FA2 . . . . FA5. This would suggest that the average hyperfine field $\langle H \rangle$, at the ^{57}Fe nuclei in these five samples depends on the process route followed, with $\langle H \rangle$ decreasing with decreasing cooling rate. It is relevant to point out that Perez Alcazar and Galvao de Silva [10] determined $P(H)$ for $Fe_{0.775}Al_{0.225}$ before and after a high temperature measurement and found a significant difference in the distributions as well as in the values of $\langle H \rangle$ and H_{peak}. These authors concluded from this observation that a partial phase decomposition occurs at high temperatures and the annealing process influences $P(H)$, H_{peak} and $\langle H \rangle$. Our present results support this conclusion. The decrease in $\langle H \rangle$ indicates a decrease in the iron magnetic moment [15] which can be attributed to an increasing electron transfer to the iron unfilled 3d bands [16]. In their Mössbauer spectroscopic studies of the alloys $Fe_{44}Ni_{36}P_{14}B_6$ Matteazi and Riontino [17] found that $\langle H \rangle$ decreases and $\langle IS \rangle$

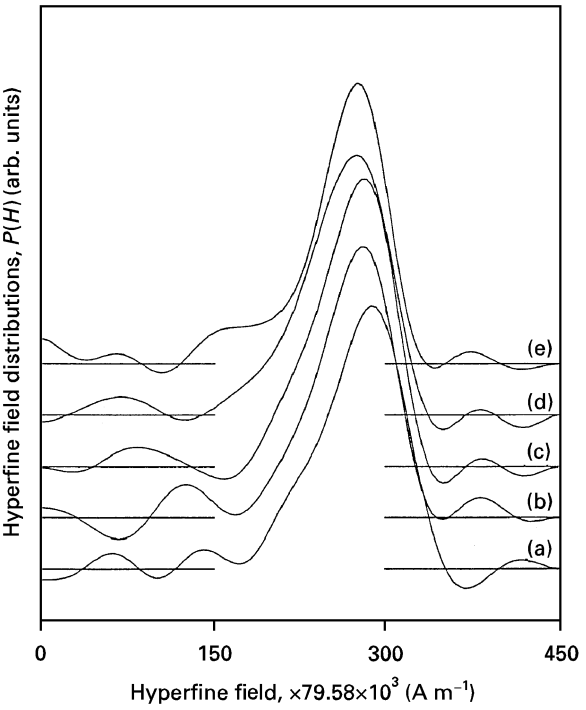

Figure 4 Hyperfine field distributions in (a) FA1, (b) FA2, (c) FA3, (d) FA4 and (e) FA5 samples.

TABLE V The results for H_{peak}, $\langle H \rangle$, ΔH_1, ΔH_2 and $\langle IS \rangle$ for the samples FA1–FA5

Sample	$\langle H \rangle$ $\times 79.58 \times 10^3$ (Am^{-1})	$\langle$IS$\rangle$ ($mm\,s^{-1}$)	$H_{peak}^{(a)}$ $\times 79.58 \times 10^3$ (Am^{-1})	ΔH	
				$\Delta H_1^{(b)}$ $\times 79.58 \times 10^3$ (Am^{-1})	$\Delta H_2^{(c)}$ $\times 79.58 \times 10^3$ (Am^{-1})
FA1	271 ± 3	0.07 ± 0.01	290	48	34
FA2	267 ± 3	0.07 ± 0.01	286	44	34
FA3	260 ± 3	0.07 ± 0.01	283	46	34
FA4	252 ± 3	0.08 ± 0.01	273	46	37
FA5	249 ± 3	0.08 ± 0.01	271	34	34

(a) H_{peak} is the most probable value of H
(b) half-width-at-half maximum on the left side of peak position
(c) half-width-at-half maximum on the right side of peak position

increases with decreasing cooling rate and that this behaviour could be understood in terms of changes in spin and charge density.

4. Summary and conclusions

The Mössbauer spectra of four samples of Fe–24 at % Al and one sample of Fe–25 at % Al have been measured at room temperature. The processing route followed in the preparation of each sample differed in respect of their heat treatment temperatures and rate of cooling so that different phases were possible. The hyperfine magnetic fields, H, associated with these phases were obtained by analysing the Mössbauer spectra and these H-values were used to identify the atomic configurations around the Fe atom. In the case of alloys containing 24 at % Al, the atomic configuration assigned for the samples were almost the same although the relative populations (i.e., volume-fraction of phases) showed some differences (except FA1 and FA2). This behaviour suggested that the nature of the processing route influenced the relative population (or volume fraction) of the phases. In the case of the alloy containing 25 at % Al (sample FA5) the configurations and the relative populations showed differences from the other four samples.

The hyperfine magnetic field distributions, $P(H)$, were determined for each sample. Apart from minor differences the distributions for the four samples (FA1–FA4) containing 24 at % Al appear similar while that for the FA5 sample containing 25 at % Al showed a different shape. The average hyperfine magnetic fields $\langle H \rangle$ and average isomer shifts determined from these results showed that these quantities depend on the heat treatment temperature and the rate of cooling.

References

1. K. VEDULA, in "Intermetallic Compounds, Vol. 2, Practice", edited by J. H. Westbrook and R. L. Fleischer (John Wiley & Sons, New York, 1994) p. 199.
2. J. C. WANG, D. G. LIU, M. X. CHEN and X. X. CAI, *Scripta Metallurgica* **25** (1991) 2581.
3. K. ONO, Y. ISHIKAWA and A. ITO, *J. Phys. Soc. Jpn.* **17** (1962) 1747.
4. M. B. STEARNS, *Phys. Rev.* **147** (1966) 439.
5. L. CSER, J. OSTANEVICH and L. PAL, *Phys. Stat. Sol.* **20** (1967) 581.
6. *Idem*, *ibid* **20** (1967) 591.
7. M. R. LESOILLE and P. M. GIELEN, *ibid* **37** (1970) 127.
8. G. P. HOFFMAN and R. M. FISHER, *J. Appl. Phys.* **38** (1967) 735.
9. I. VINCZE and L. CSER, *Phys. Stat. Sol.* **50** (1972) 709.
10. G. A. PEREZ ALCAZAR and E. GALVAO DA SILVA, *J. Phys. F: Met. Phys.* **17** (1987) 2323.
11. E. P. YELUSOV, E. V. VORONINA and V. A. BARINOV, *J. Magn, Magn. Mater.* **115** (1992) 271.
12. O. KUBASHEWSKI, "Iron-binary phase Diagrams", (Springer-Verlag, Berlin, 1982), p. 5.
13. U. GONSER and M. RON, in "Applications of Mössbauer spectroscopy", Vol. II, edited by R. L. Cohen, (Academic Press, New York, 1980) p. 281.
14. B. WINDOW, *J. Phys.* **E4** (1971) 401.
15. P. PANISSOD, J. DURAND and J. I. BUDNICK, *Nucl. Instr. Methods* **199** (1982) 99.
16. K. YAMAUCHI and T. MIZOGUCHI, *J. Phys. Soc. Jpn.* **39** (1975) 541.
17. P. MATTEAZZI and G. RIOUTINO, *Hyperfine Interactions* **28** (1986) 971.

Received 23 July 1996
and accepted 17 June 1997